Silicon (2021) 13:2319–2335
https://doi.org/10.1007/s12633-020-00812-8

ORIGINAL PAPER

Physico-Mechanical Properties of Nano Silica-Filled Epoxy-Based Mono and Hybrid Composites for Structural Applications

B. Suresha[1] · G. S. Divya[1,2] · G. Hemanth[3] · H. M. Somashekar[4]

Received: 31 July 2020 / Accepted: 27 October 2020 / Published online: 24 November 2020

Abstract

This research article describes the results of nano-silica ($nSiO_2$) filled epoxy (Ep) mono composites with different contents (0.5, 1.0, 1.5, 3, and 5 wt.%) and carbon fabric-reinforced epoxy (CFE) with 1.5 and 3 wt.% of $nSiO_2$ hybrid composites and their physical and mechanical properties characterized by different techniques as per ASTM standards. Mechanical mixing and sonication techniques were followed to disperse $nSiO_2$ into Ep resin. Furthermore, the same $nSiO_2$/Ep is reinforced with carbon fabric by hand lay-up followed by vacuum-bagging technique. The morphological features were studied by scanning electron microscopy. The properties of the Ep based mono and hybrid composites showed that the hardness, tensile strength/modulus, and flexural strength/modulus, as well as impact strength of the composites enhanced with $nSiO_2$ wt.% up to 3 wt.% for mono and hybrid composites and decreased thereafter; suggesting that the beneficial properties ensued up to 3 wt.% $nSiO_2$ content.

Keywords Nano silica · Mono and hybrid composites · Vacuum bagging technique · Mechanical properties · Fracture morphology

1 Introduction

The composites materials are the heterogeneous material that has gained acceleration in development, testing, and application of composites for various engineering applications like structural, aeronautical, automotive, tribological, thermally conductive, electrical insulations, packaging and so on [1–3]. Out of these applications, all of them have a unique requirement that cannot be met by the conventional metallic and alloyed components. Hence, the composites are introduced to modify the materials for the specific requirements without changing their base functionalities. The heterogeneous mixture of the composites allows the materials to contribute individually to the overall performance of the materials. The composites are classified into three types based on the host materials; they are, metal matrix, ceramic matrix, and polymer matrix composites. The polymer matrix is further classified into the thermoplastic and thermoset plastic matrices. Thermoset polymers are more advantageous upon comparing with thermoplastics. The positive aspects of thermoset resins are ease of fabrication, faster curing, chemical retardant, flame retardant, holds the structural integrity even when heated, and so on. This article deals with one such polymer, epoxy. There is a lot of research that had been conducted over the years on properties and behaviour of epoxy under different operating conditions [4–7]. Even though there is a lot of research conducted on epoxy, still there are various avenues to explore the epoxies for engineering applications. Hence, Epoxy was selected as a host material in the current investigation.

The thermoset resins are brittle and to improve its properties still further reinforcements are being introduced along with matrix. The reinforcements are available in the forms they are fibers, particulates, whiskers, flakes. Again, fibers are classified as short fibers and long fiber woven fabrics. Particulates are available in various geometry layered, spherical, tubular, random shaped powders. These particulates also vary in their dimension. It can range from nanometres to a few 100 μm. In this study, both fibers and particulates are incorporated and studied. There are a lot of fibers available for the research community to carry out research. To name a few

✉ B. Suresha
sureshab@nie.ac.in

[1] Department of Mechanical Engineering, Centre for Composite Materials Research, National Institute of Engineering, Mysuru, India

[2] Department of Automobile Engineering, Dayananda Sagar College of Engineering, Bengaluru, India

[3] EAI-4 Department, Robert Bosch Engineering and Business Solutions Pvt Ltd, Bengaluru, India

[4] Department of Mechanical Engineering, Dr. Ambedkar Institute of Technology, Bengaluru, India

carbon fibers, glass fibers, aramid fibers, basalt fibers, boron fibers, and the recent trend is the usage of natural fibers like pineapple fibers, banana fibers, flax fibers, jute fibers and so on [3, 4, 8, 9]. However, for the structural application scenario, the natural fibers are still under developing stage to meet the high strength to weight ratio demands of the engineering applications. So, the researchers are continuing with the synthetic fibers to meet the demand. The carbon fibers are promising in enhancing the overall physico-mechanical properties of the host matrix. The carbon fibers have proved to have very strength to weight ratio making them feasible for aerospace applications that have limited factor of safety. The carbon fibers are compatible with both thermoplastics; mostly they are used as short fiber reinforcements [10, 11]. Although, the flexibility of thermoset polymers, offered the choice to utilise both the short fibers and woven fabric mats [12, 13]. Owing to these benefits of carbon fibers in enhancing the mechanical properties for structural applications, the carbon fiber was introduced as reinforcement in this study. However, there is one more possible combination for the fabrication of two-phase material that is using Nano particulates with epoxy. In this sense, there is an innumerable amount of nanoparticles that are being prepared for various activities like medical, engineering, and other applications. The nanoparticles are prepared from allotropes of carbon (Graphite, graphene, carbon nanotubes), metals and metal oxides (TiO_2, SiO_2, Al_2O_3, $CaCO_3$, iron nanoparticles, gold nanoparticles, molybdenum disulfide, copper-based particles and so on) and other ceramic nanoparticles like boron nitride, boron carbide, Nano clay and so on.

Researchers have used different nanoparticles to impart better strength and toughness to the materials. Nanoparticles that are well blended will penetrate between the fibers and form strong bonding. Kaybal et al. [14] have incorporated Al_2O_3 with CFE composites and found low energy absorption and the highest damage resistance. Nallusamy [15] investigated the flexural property of the glass fiber (GF)/Epoxy (GFE) composites. They observed the strength got enhanced at 3 wt.% of TiO_2. SiO_2 with GFE composites and found the SiO_2 in aiding the improvement in tensile strength at 1 wt.% of SiO_2. They also discussed that, the $nSiO_2$ particles enhances the compatibility with the polymer chains and presents very high chemical reactivity [16]. Yang et al. [17] have incorporated the 1 wt.% $nSiO_2$ particles with the GFE composites and found improved tensile properties. There are works involving the $nSiO_2$ with epoxy as the two-phase composites [18–23]. The degree of crystallinity of epoxy gets affected by the addition of the $nSiO_2$ was discussed in detail with the help of differential scanning calorimetry [18]. The addition of the $nSiO_2$ will lead, not only to improve the mechanical and tribological properties but it also observed stability in the thermal properties [23]. Table 1 shows the literatures that have used $nSiO_2$ as nanoparticle reinforcement. The $nSiO_2$ has proved its role in improving the properties of the composites. The effect of the silane treatment on improving the adhesion and ease of dispensability has made $nSiO_2$ a potential nano additive for the composite. Hence, in this investigation, $nSiO_2$ was incorporated with the CFE composites to study the mechanical properties and analyse the fracture surface morphology.

The main goal of this article is to study the physico-mechanical properties of the epoxy-based mono and hybrid composites. Prepared composites were of two types firstly, two-phase $nSiO_2$/Ep and secondly three-phase $nSiO_2$/CFE composites. Prepared materials' density, Barcol hardness, tensile, flexural, and impact properties were investigated according to governing ASTM standards. Finally, the specimens that are failed under the static and impact loading were analyzed under a scanning electron microscope to study the fracture surface morphology.

2 Experimental Details

2.1 Materials

Araldite LY1564 epoxy resin and Aradur 22,962 hardener procured from Huntsman Ltd. were used in the mono and hybrid composites fabrication. The density of the epoxy was 1.1–1.2 g cm^{-3} and that of the hardener was 0.8–0.9 g cm^{-3}. The mixing of resin to hardener weight proportion was 100:25 as prescribed by the manufacturer. T300 plain carbon fabric with a low density of 1.76 g cm^{-3} and high tensile strength of 3.5 GPa and Young's modulus of 230 GPa procured from CF composites, New Delhi, India was used as reinforcement in the hybrid composites. The areal mass of the carbon fabric is 200 GSM. The $nSiO_2$ was procured from Sigma Aldrich Ltd., India. The dimension of the $nSiO_2$ was 10–20 nm. The powder $nSiO_2$ has a density of 2.2 to 2.6 g cm^{-3} at 25 °C as per the manufacturer data sheet.

2.2 Preparation of Composites

2.2.1 Fabrication of Epoxy Mono-Composites

Surface modification of fiber, particles, and resin enhances the bonding between the constituents by removing the impurities and hydroxyl group present over them and it helps in uniform dispersion of particles in the resin. Therefore, the epoxy resin was treated using amine containing liquid rubber hydroxyl terminated polycis-butadiene (HTPB) and the treatment of SiO_2 particles was carried out using silane-coupling agent (KH560). The benefits of the silane treatment were reported in many literatures [23, 27]. The epoxy-based mono-nanocomposites were prepared by combining treated $nSiO_2$ filler with a pre-weighed amount of epoxy and a tiny amount of

Table 1 Summary of the literature on composites with $nSiO_2$ filler

Materials	Conditions	Remarks	Publication
$nSiO_2$ + Epoxy	Mechanical stirring at 60 °C.	The curing kinetics, material properties and the failure surface morphology were examined. The aggregates free state at very high loading of nanoparticles.	Liu et al. [24]
nSiO2 + Epoxy	$nSiO_2$ was treated with silane and alcohol.	Usage of Acetone in dispersion process was reported in this article. The filler loading in this article ranged from 1 wt.% to 5 wt.%. Improvement in mechanical properties was maximum at 3 wt.%. Tribological benefits and thermal stability were reported.	Zhu et al. [23]
nSiO2 + PBT + Epoxy	$nSiO_2$ was treated with silane	The Melt blending process (through twin extruder) was incorporated for the fabrication of the composites. Benefits in phase morphology and mechanical properties were reported.	Zhang et al. [25]
nSiO2	The epoxy was heated to reduce the viscosity and ultrasonicated to disperse $nSiO_2$. Specimens were polished.	Extent of dispersion was proved by presenting the TEM micrographs. The linear relationship between fracture toughness and fracture load were investigated. Digital Speckle correlation method was also incorporated to discuss the deformation phenomenon of matrix.	Yao et al. [26].
$nSiO_2$ + Epoxy	The Silane treatment was used to aid the $nSiO_2$ dispersion.	The physical and mechanical properties were performed and the ANOVA was introduced to find the optimum loading of the $nSiO_2$ in epoxy.	Nijke et al. [27]
$nSiO_2$ + Epoxy	Polymer grafting was performed on $nSiO_2$ and dispersion is through the solvent dispersion.	The mechanical properties, fatigue and the fracture behaviour were investigated and the roles of PHMA and PGMA on improving the properties were studied in detail. PHMA block produced the growth of void and the shear banding. However, PGMA improved the properties by supporting the blending.	Gao et al. [28]
MWCNTs+ CFE	Different stitching pattern of the carbon fabric.	The failure of the composites under flexure is usually because of matrix cracking, debonding of the layers and warp fiber breakage.	Bilisik et al. [13]
Carbon fiber+Epoxy	Different cure pressure (0 to 0.4 MPa).	The deterioration of the composite tensile property due to the void content increased with reduction in cure pressure.	Zhu et al. [12]
$nSiO_2$ + Glass fiber+ Epoxy	The ultrasonication process with only 65% amplitude was incorporated	The influence of $nSiO_2$ on tensile properties was discussed for with the experimental investigation. Along with the experimentation, the imperialist competitive algorithm was utilized to model the mechanical property as a polynomial equation of fourth degree.	Feli and Jalilian [29]
$nSiO_2$ + short carbon fiber+Epoxy	High energy vacuum dissolver was used for dispersion. Double stage cooling	The stress state near the micro sized particles to nano sized particles were reported and role of plastic zone near the crack tip on the properties of composites were reported. Micro cracks were observed near the SCFs.	Zhang et al. [30]
$nSiO_2$ + GO+carbon fiber+Epoxy	Vacuum assisted resin transfer molding was used.	The adhesion of the $nSiO_2$/GO films on to the carbon fibers were discussed in details. The benefits of this adhesion process improving the interfacial properties of the polymer/fiber bonding in the composites were reported along with the improvement in the properties between untreated composites to treated composites.	Fu et al. [31]
$nSiO_2$ + carbon fiber +Epoxy	The ammonia / ethylene plasma treatment on the fibers were performed before fabrication process	The influence of the plasma treatment on the carbon fibers in improving the mechanical properties. Specifically this article deals with the interfacial shear strength.	Lew et al. [32]

acetone at 26 °C with sonication for 2 h to distribute the nanoparticles consistently within the epoxy matrix material [23]. Then the sonicated mixture was heated to 60 °C for 30 min to remove the acetone fully. Moreover, the curing agent was added with stirring for 3 min. Finally, the mixture was transferred to aluminum mould and degassed at 60 °C for 1 h to remove air bubbles in a vacuum oven. For curing the composites, the heating and cooling rate was 5 °C /min and 1 °C /min respectively. Figure 1 shows the time-temperature profile for the curing of the epoxy mono-composites.

2.2.2 Fabrication of Nano Silica-Filled Carbon Fabric Reinforced Epoxy Hybrid Composites

The fabrication of nano silica-filled carbon fabric reinforced epoxy (CFE) hybrid composites is an extension of the

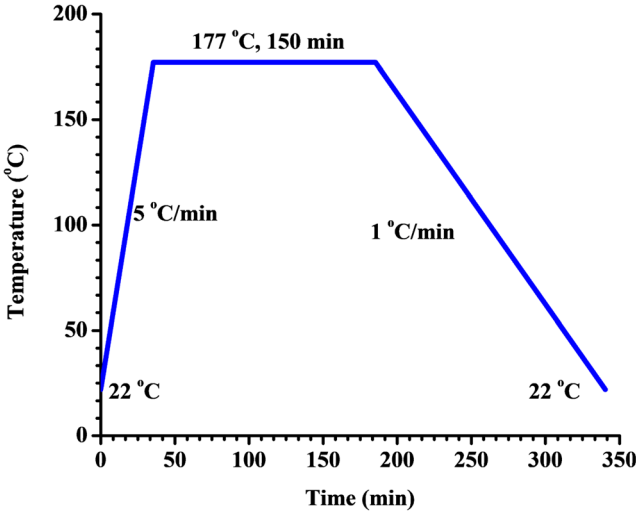

Fig. 1 Time-temperature characteristics for the curing of epoxy mono-composites

fabrication of mono composites. The same procedure as discussed in 2.2.1 was used to blend the $nSiO_2$ with epoxy. The carbon fiber fabrics received from the supplier were further treated with silane coupling agent. The as received carbon mat were cleaned with a deionized water and post open air drying the acetone solution cleansing was incorporated in order to remove the unwanted impurities and surface polarities. Later, it was dried in a vacuum assisted hot drier at a temperature of 100 °C in a vacuum for 4 h. For the silane treatment of the carbon fiber fabric, the procedure mentioned by Zegaoui et al. was followed [33]. The 0.9 g of the silane agent was dispersed in the 60 ml of ethanol and 40 ml of deionised water. Electric stirrer for about 5 min stirred the solution then fibers were treated with the resulting solution. Fibers were washed again with acetone solution to remove the excessive silane. Later, the fibers are dried again in a vacuum drier at 100 °C for 10 h. This carbon fiber fabric was taken further. The hand lay-up of hybrid composites is prepared as per the composition listed in Table 2 and transferred into vacuum bagging set up. Vacuum pressure of 1 atm was applied for about 2 h. Later the composite laminates were cured at the room temperature for 24 h and the post-curing operation was performed at 100 °C for about 1 h in an air circulated oven. Figure 2 shows the details of the fabrication process.

2.3 Test Procedure Followed for Epoxy Based Mono and Hybrid Composites

Prepared composites were tested for the physico-mechanical properties following the governing ASTM standards. The test was initiated with a density test as per the ASTM D 792 standard with a specimen dimension (6 mm × 6 mm × 3 mm). Theoretical density and the void content in the composites were calculated using Eq. 1 and 2 respectively [34]. The hardness was tested according to ASTM D 2583 using Barcol hardness tester. The tensile test was performed according to ASTM D638 with a crosshead speed of 5 mm min^{-1}. The flexural test was performed as per the ASTM D 790 standard by keeping the length to thickness ratio as 20 and crosshead speed of 2.5 mm min^{-1}. Both tensile and flexural properties were performed using 100 kN UTM from Kalpak Instrument, Pune, India. The impact test was according to ASTM D 256–10. The total specimen length was 60 mm. the width was 12 mm and a notch was made at the centre of the specimen to a depth of 1.84 mm that led to the final width of 10.16 mm. Finally, an impact test was done and the energy absorbed was recorded. The R3 hammer (10.84 J) was used for impacting in a cantilever beam impact-testing machine. The pendulum hammer used here travelled at a speed of 3.46 ms^{-1} to hit the specimen during the test. The energy absorbed by the composites was considered as a measure to scale the impact strength of the material. All tests were repeated five times to get a mean value of the specimen.

$$\frac{1}{\rho_{Theoretical}} = \frac{W_{fiber}}{\rho_{fiber}} + \frac{W_{filler}}{\rho_{filler}} + \frac{W_{matrix}}{\rho_{matrix}} \quad (1)$$

$$Void\% = \frac{\rho_{Theoretical} - \rho_{Actual}}{\rho_{Theoretical}} \times 100 \quad (2)$$

Table 2 Composition of the fabricated mono and hybrid composites

Composite Code	Carbon fiber (wt.%)	Epoxy matrix (wt.%)	$nSiO_2$ particles (wt.%)
E100	–	100	–
E99.5/$nSiO_2$–0.5	–	99.5	0.5
E99/$nSiO_2$–1	–	99	1
E98.5/$nSiO_2$–1.5	–	98.5	1.5
E97/$nSiO_2$–3	–	97	3
E95/$nSiO_2$–5	–	95	5
C60/E40	60	40	–
C60/E38.5/$nSiO_2$–1.5	60	38.5	1.5
C60/E37/$nSiO_2$–3	60	37	3

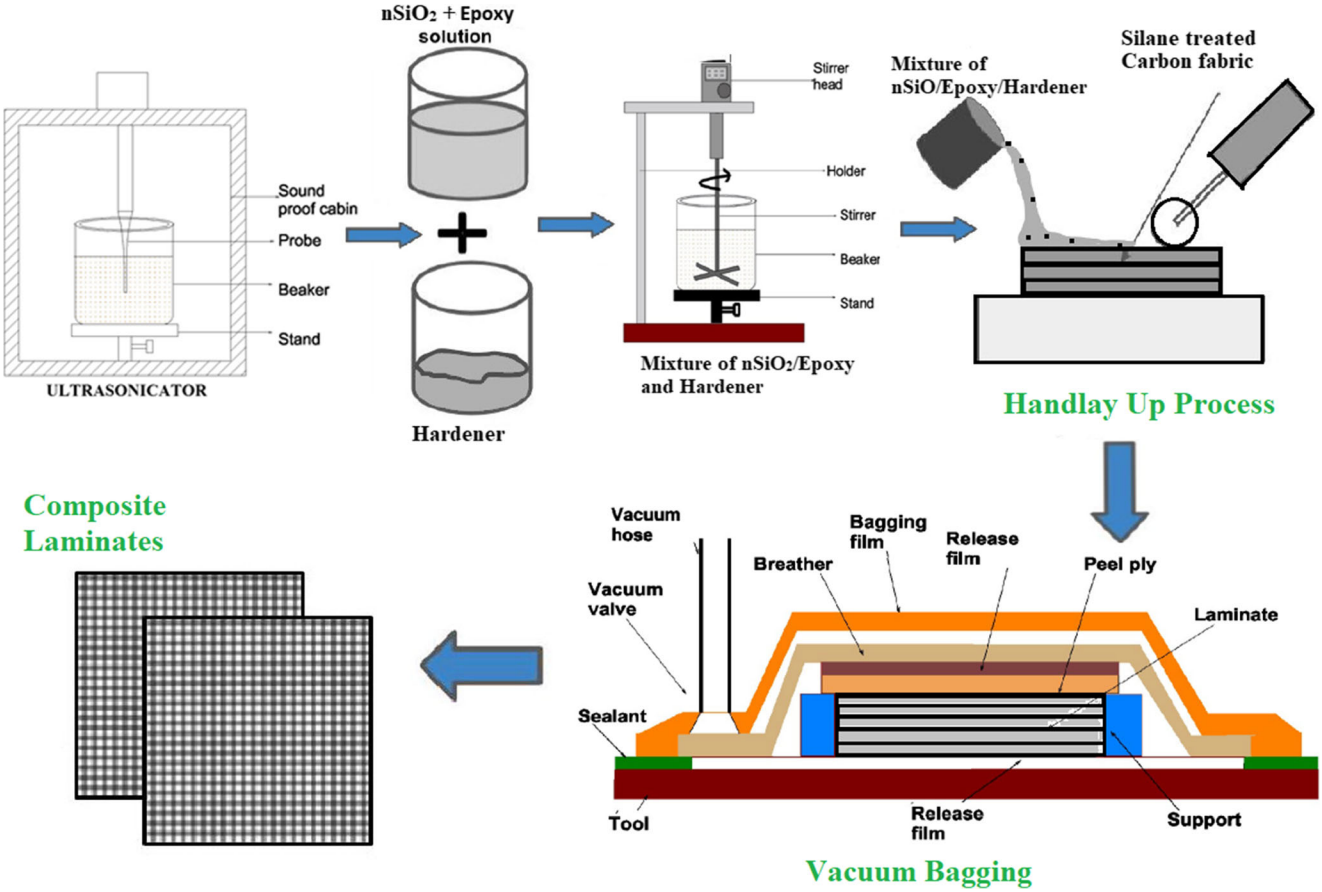

Fig. 2 Detailed scheme for the fabrication of the CFE hybrid composites

where,

$\rho_{Theoretical}$, ρ_{Actual}	Theoretical and actual density of the composites
ρ_{fiber}, ρ_{filer}, ρ_{matrix}	Densities of fiber, filler, and matrix
W_{fiber}, W_{filler}, W_{matrix}	Weight fraction of fiber, filler, and matrix.

2.4 Microscopy

Transmission electron microscopy (TEM, model JEOL 1200 EX, Japan) with standard magnification was utilized to examine the scattering of $nSiO_2$ particles in the epoxy matrix composites at an acceleration voltage of 100 kV. TEM coupons were prepared utilizing a ultra-microtome (Ultracut-1, UK) with a diamond saw, and the sectioned coupons (ca. 70 nm in thickness) were set in 200 mesh copper grids for perception. Furthermore, scanning electron microscopy (SEM, JEOL JSM-6480LV, Japan) was utilized to investigate the fiber/filler dispersions, the interaction between fiber and epoxy matrix, as well the fractured features of CFE hybrid composites. The fractured surfaces were sputter coated with gold to enhance the conductivity.

3 Results and Discussion

3.1 Effect of Nano Silica on Density and Hardness of Epoxy Based Mono and Hybrid Composites

Gradual increment in the composites' density is the attribute of the bulk density of the $nSiO_2$, which is higher than epoxy and the carbon fiber. The highest density was noted at 5 wt.% of the $nSiO_2$ filled composite among mono composites and hybrid composites, 3 wt.% filled CFE. An important point to be noticed here is that for every 0.5 wt.% increase in the $nSiO_2$ in the composites, the density was enhanced by 0.002 g cm^{-3}. This linear relation was observed until 3 wt.%. Beyond this, the trend deviated. Table 3 shows the summary and Fig. 3a-b depicts the density of the composites for the Epoxy/$nSiO_2$ mono and CFE /$nSiO_2$ hybrid composites. However, the trend after the addition of the filler in neat epoxy and CFE remained the same. A similar linearity relationship was noticed in several research papers [17]. Table 3 and Fig. 3c shows the void content in the material has an increasing behaviour in non-fibrous composites and it has a decreasing behaviour in the $nSiO_2$/CFE composites. The voids are created due to the air entrapment in the epoxy and also the improper degasification. The adverse effect of these void contents is the reduction in

Table 3 The density and void content of the $nSiO_2$/Ep and $nSiO_2$/CFE composites

Composites	Theoretical density (g cm^{-3})	Experimental density (g cm^{-3})	Void content (%)
E100	1.15	1.149 ± 0.05	0.93
E99.5/$nSiO_2$–0.5	1.1790	1.161 ± 0.04	1.36
E99/$nSiO_2$–1	1.1808	1.163 ± 0.05	1.51
E98.5/$nSiO_2$–1.5	1.1833	1.165 ± v0.07	1.55
E97/$nSiO_2$–3	1.1881	1.169 ± 0.04	1.61
E95/$nSiO_2$–5	1.2067	1.175 ± 0.06	2.63
C60/E40	1.513	1.49 ± 0.005	1.52
C60/E38.5/$nSiO_2$–1.5	1.523	1.50 ± 0.004	1.506
C60/E37/$nSiO_2$–3	1.5369	1.52 ± 0.007	1.11

the properties of the material. Various researchers [12, 22, 35] experimentally affirmed these effects. The neat epoxy composite had void content of 0.8% and it increases to 1.4% with E99.5/$nSiO_2$–0.5, 1.53% with E99/$nSiO_2$–1, 1.62% with E99/$nSiO_2$–1.5 and 1.71% with E97/$nSiO_2$–3 and 2.73% with E95/$nSiO_2$–5. However, CFE composites the void content reduced from 1.6% to 1.53% for C60/E38.5/ $nSiO_2$–1.5 and 1.09% with C60/E37/ $nSiO_2$–3.

The increment in the hardness with respect to filler loading was the effect of indentation location. When indentation is

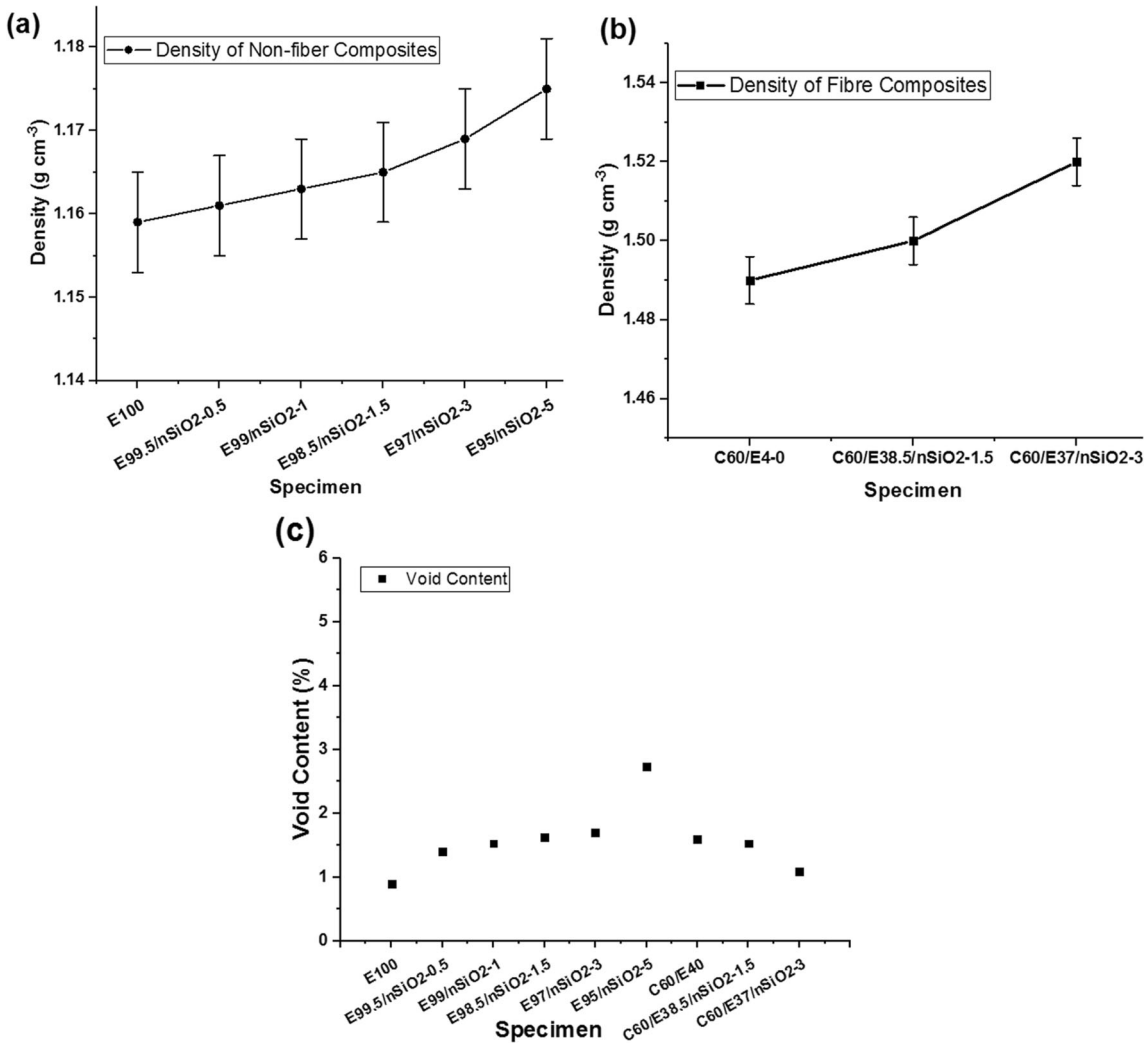

Fig. 3 The plot of the density and void content of the composites: **a** Epoxy/$nSiO_2$ mono composites, **b** CFE/$nSiO_2$ hybrid composites, **c** Void content of mono and hybrid composites

made under the compression loading the polymer, fiber, and the particle within the periphery of the indenter get compressed and resists the indenter from going down a little deeper. This gives rise to higher hardness [10, 36]. For obtaining the optimum result, ten indentations were made all over the composite palette and the average was noted. Hence, it was concluded that the superior dispersion of the nanoparticle dictates the overall hardness of the material. Liu et al. investigated the augmentation of the hardness of the material through the atomic force microscopy and they justified that the denser crosslinking of $nSiO_2$ and epoxy leads to the improvement in the localised hardness and that eventually improved overall hardness of the composites. [1]. upon incorporation of fibers to the epoxy/$nSiO_2$, mixture increased the hardness by 7.84%. Figure 4 shows the hardness of the composites. A similar trend was observed in research works elsewhere [37, 38].

3.2 Effect of $nSiO_2$ on Tensile Properties of Epoxy Based Mono and Hybrid Composites

The addition of SiO_2 was found to be beneficial in augmenting the tensile strength and modulus. The host epoxy has a tensile strength and modulus of the 50.52 MPa and 2.82 GPa. Whereas, the E99.5/$nSiO_2$–0.5 increased tensile property by a very small quantity (50.98 MPa and 2.83 GPa). The small quantity of the SiO_2 might act as a stress concentration region this might initiate the localized cracks that prevent the composite from having an increase in the properties. With E99/$nSiO_2$–1, the tensile strength had a steep enhancement of 23.61% however, the tensile modulus incremented only by 2.12%. The strength enhancement between the E99/$nSiO_2$–1 and E99/$nSiO_2$–1.5 was 1.58%. The highest increment in the tensile property was observed with E97/$nSiO_2$–3 of the SiO_2 with a tensile strength of 66.45 MPa and 3.12 GPa. Better dispersion order of the particles restrains the load flow more efficiently [39]. With further loading of the SiO_2 yielded no benefits in improvement in tensile properties. After a certain loading of nanoparticles, poor dispersion quality will be seen due to the agglomeration of particles. This deteriorates the tensile strength [19, 20, 40, 41]. The values of the tensile strength, modulus, and elongation at fracture are plotted in Fig. 5a-c. Increment in the modulus was not as high as the strength as observed in Chen et al. [21] work. Suresha and Saini [42] have incorporated the nano montmorillonite with CFE composites and found the increment in the tensile properties for the 5 wt.% of the nanoparticle loading. Zhou et al. [43] attributed the decreased tensile strength to the formation of the localized stress states.

The incorporation of the carbon fiber with epoxy increased the ultimate tensile strength by 10.26 folds and modulus by 7.29 times. With C60/E38.5/ $nSiO_2$–1.5 the strength was increased by 3.33% and modulus was increased by 6.55%. Similarly, C60/E37/ $nSiO_2$–3 the strength was increased by 13.87% and the modulus was increased by 16.69% concerning neat epoxy. The increased fiber-matrix interaction due to good adhesion resulted in increasing the tensile strength and modulus with a fibrous composite system. The void content decrement also has a part to play in improvement in tensile properties with $nSiO_2$/CFE composites. Feli and Jalilan [29] have observed that 1 wt.% has the highest tensile strength and tensile modulus with both two-phased $nSiO_2$/Epoxy and $nSiO_2$/GFE composites.

The elongation at fracture was also captured during the testing. The host epoxy had an elongation of 2 mm. Upon addition of SiO_2 to epoxy, the elongation at break got augmented this signifies the increment in the elastic nature of the composites. With E99.5/$nSiO_2$–0.5, 0.8 mm of improvement was observed in elongation at fracture. However, further loading enhanced the elongation further. The highest elongation of

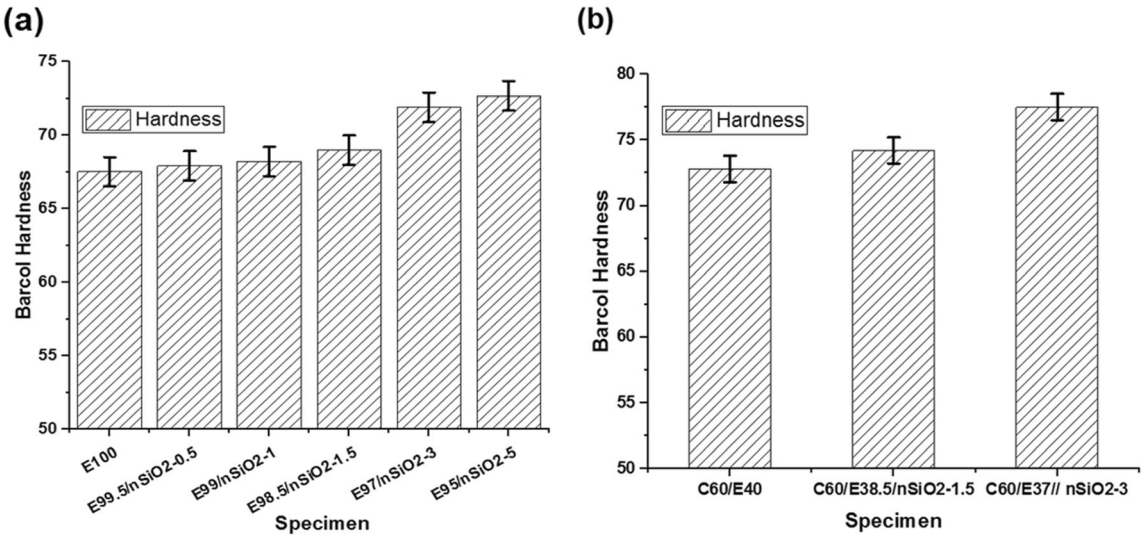

Fig. 4 Barcol hardness of the composites: **a** Epoxy/$nSiO_2$ mono composites, **b** CFE/$nSiO_2$ hybrid composites

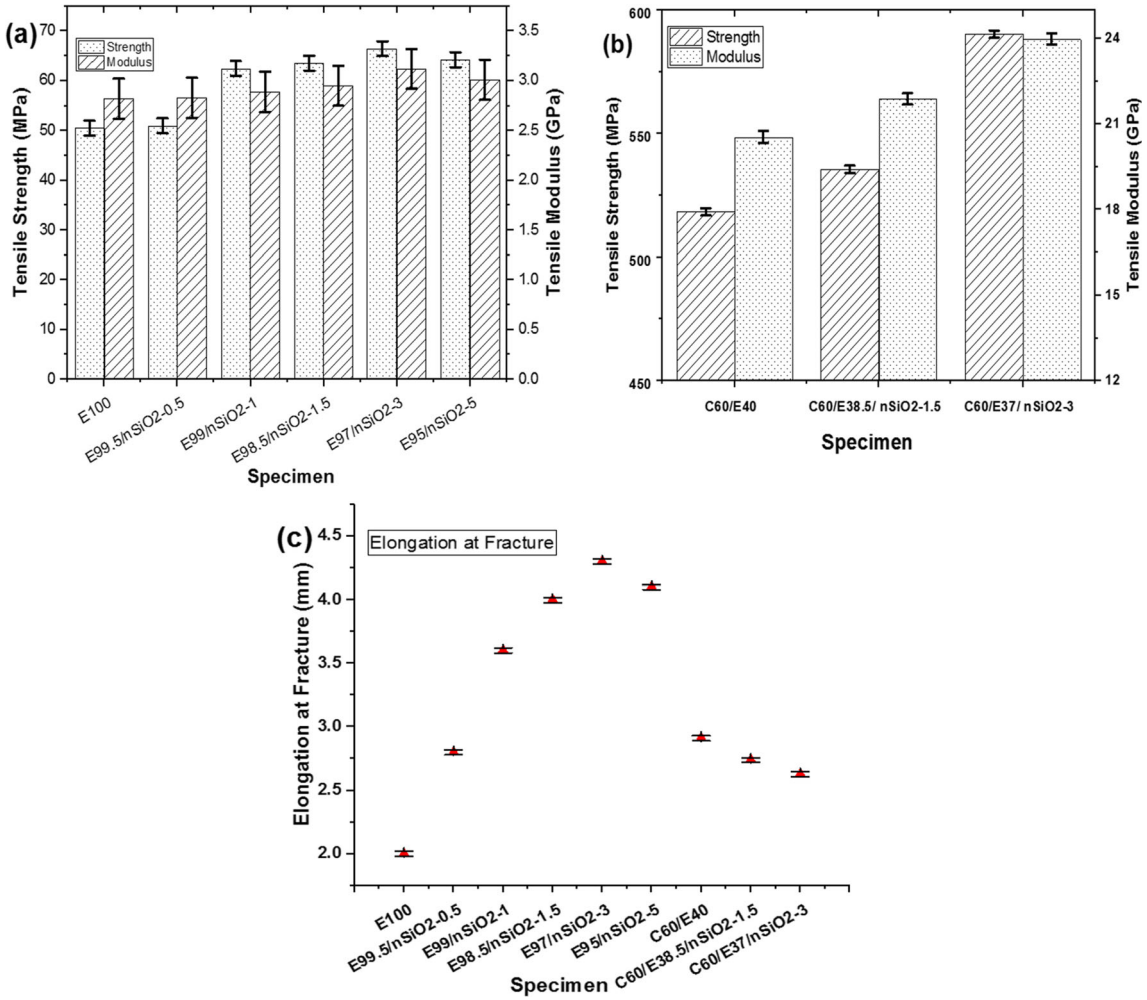

Fig. 5 Tensile properties of the composites: **a** Epoxy/nSiO_2 mono composites, **b** CFE/nSiO_2 hybrid composites, **c** Elongation at fracture of all composites

4.3 mm was observed with E97/nSiO_2–3 but with E95/nSiO_2–5 the elongation was 4.1 mm. The reason that can be attributed to the reduction of elongation at fracture is the formation of aggregates that will not participate in the load-bearing. Eventually, this reduces the strength and makes the elongation smaller by easy propagation of the locally induced cracks. The nSiO_2/CFE composites have the toughening mechanism that is observed with increasing loading of nSiO_2. This can be justified by a reduction in elongation at fracture. The unfilled CFE composite had an elongation of 2.91 mm whereas, the C60/E38.5/ nSiO_2–1.5 had an elongation of 2.74 mm and with C60/E37/ nSiO_2–3, the elongation was the least and the value is 2.63 mm. With the addition of nSiO2 particles in fibrous epoxy composites, good tensile properties can be achieved [17, 38]. Zhou et al. [43] have observed the pronounced elongation with the addition of the carbon nanofiber with 2 wt.% in CFE composites. Feli and Jalilan [29] have observed the noteworthy improvement in the elongation upon the addition of nSiO_2 with the nSiO_2/Epoxy and nSiO_2/GFE composite.

3.3 Effect of nSiO_2 on Flexural Properties of Epoxy Based Mono and Hybrid Composites

The three-point bend test was performed to seek the flexural properties of Epoxy/nSiO_2 and nSiO_2/CFE composites. The addition of the nSiO_2 improved the flexural strength in both cases. The host epoxy has the flexural strength and modulus of 98.58 MPa and 3.55 GPa whereas, the property increment of 7.41% and 1.12% was with E99.5/nSiO_2–0.5, 32.43% and 12.11% with E97/nSiO_2–3 were observed. However, further loading of the nSiO_2 yielded no benefits. Higher filler loading reduces the wettability and interlocking between the constituents leading to a reduction in properties [39]. As the carbon fiber was introduced with nSiO_2/epoxy, the flexural strength and modulus were increased by 6.85 times 7.64 respectively. The strength was enhanced with the addition of the nSiO_2 by 3.7% with 1.5 wt.% and 7.38% with 3 wt.%. However, the flexural modulus got decreased with the n-SiO_2 to CFE composites unlike to the non-fibrous composites by 14.65%. The

increased flexural property with the non-fibrous system is because of the increased stiffness of the composites. This increases the load-bearing capacity of the composites that increases the slope of the load-deflection curve increasing the strength. The increased fiber-matrix adhesion is the main reason for the improvement in the flexural strength. The reason for the increment in the strength and modulus in the non-fibrous composite system is very much dependent on the modulus of the $nSiO_2$ particles [44]. Improvement is because of interfacial adhesion between the fiber and matrix and the internetworking of the polymer that seizes to exist when a particle filling crosses a certain level [45]. Surface modification and fabrication processes also a factor in assessing the material properties [46]. Modification through several chemical treatments improves interfacial bonding and enhances the flexural properties [47]. The deflection at fracture was observed to increase with the addition of the $nSiO_2$ with epoxy. This increment is about 14.28% with the E99.5/$nSiO_2$–0.5, 39.28% with E99/$nSiO_2$–1, 50% with E98.5/$nSiO_2$–1.5, 60.51% with E97/$nSiO_2$–3 and 67.58% with E95/$nSiO_2$–5. The enhanced deflection was observed until E97/$nSiO_2$–3 with epoxy in the studies performed due to maximum adhesive force among the various materials in the composite [48]. Further filler loading, failed in transferring load uniformly, in turn, localized stresses were developed. This leads the material to fracture [17]. Figure 6a-c illustrates the effect of the addition of $nSiO_2$ particles.

3.4 Effect of $nSiO_2$ on Impact Strength of Epoxy Based Mono and Hybrid Composites

The impact strength is an intrinsic property of the material that resists the material from suddenly applied load. The $nSiO_2$ infused into the epoxy matrix has significantly influenced the impact strength. The host epoxy has an impact strength of 99.56 J/m. Upon, infusion of 0.5 wt.% of the $nSiO_2$ the impact strength was enhanced by 2.79%, with E99/$nSiO_2$–1, 6.7% of enhancement was observed with the impact strength. With E98.5/$nSiO_2$–1.5 and E97/$nSiO_2$–3, the increments were 13.28% and 20.98%. However, the better impact resistance was observed with E99.5/$nSiO_2$–0.5 that is 23.04%. The improved impact resistance is because of the uniformity in dispersion. The crack propagation was resisted by nanoparticles that are dispersed. The effects of the aggregates cannot be neglected because the increment in the impact strength between the consecutive loadings is higher when compared to the increment between 3 wt.% and 5 wt.%.

The second part of the investigation deals with the impact performance of the composites with fiber reinforcements. The host epoxy has an impact strength of 99.56 J/m. With 60 wt.% of the fibers the impact strength augmented by 24.55 times. The incorporation of 1.5 wt.% of SiO_2 enhanced the impact resistance by 1% and 3 wt.% of $nSiO_2$ increased the impact of resistance by 1.8%. This is very negligible when compared to the increments observed in non-fibrous systems. Figure 7a shows the variation in the impact strength for the non-fibrous composite system and Fig. 7b shows the variation in impact strength with the fiber system. Higher impact energy seen in the composites is mainly because of the rigid $nSiO_2$ particles addition [47–49].

The impact is made on a notched specimen in a transverse direction. The crack propagation in the specimens subjected to impact force is directly dictated by the resistance offered to crack propagation. It is a well-known fact that the cracks propagates in a path of the least resistance. The host epoxy showed the least impact strength because of the lack of obstacle for the crack propagation. However, upon incorporation of the $nSiO_2$ to host matrix, it offered incremented amount of resistance that is evident from the plot in the Fig. 7. Although, there is an increment in energy absorption after incorporation of $nSiO_2$ with epoxy, the resistance for the impact load is not sufficient to use that in an engineering application. Hence, the addition of the carbon fibers made the composites much stronger towards the impact loads. Figure 8a pictorially depicts the crack propagation through neat epoxy. Crack propagates in different directions and almost linearly through the matrix due to the lack of the resistance. However, the cracks travelled in different directions but still managed to be in a same plane. In Fig. 8b, incorporation of $nSiO_2$ try to induce the certain amount of the resistance for the propagation of the crack. However, this is dependant over a degree of dispersion of $nSiO_2$ and on the adhesion between the nanoparticles and epoxy. Hence, the usage of silane compound was justified.

If aggregates are formed, there is a probability of the cracks propagating easily around the large aggregates or it may also break the aggregate and pass right through it. Hence, the addition of the carbon fibers led to substantial increment in the impact strength. The impact on the fibrous composites is unlike the non-fibrous composites as the majority of the energy is absorbed to break the carbon fiber whereas, the crack propagates in the same fabric layers as there is no other medium to offer resistance as depicted in Fig. 8c. In Fig. 8d, the crack propagated through not only the same carbon fiber layer but also, it get also through the different fabric layers. In this process, the $nSiO_2$ tend to absorb energy as there is a good adhesion between the epoxy and $nSiO_2$.

3.5 Morphology and Fractography of Epoxy Based Mono and Hybrid Composites

3.5.1 Morphology and EDAX of Epoxy Based Mono Composites

The studies on the mechanical properties of the composites that are reinforced with the nanoparticles are highly influenced

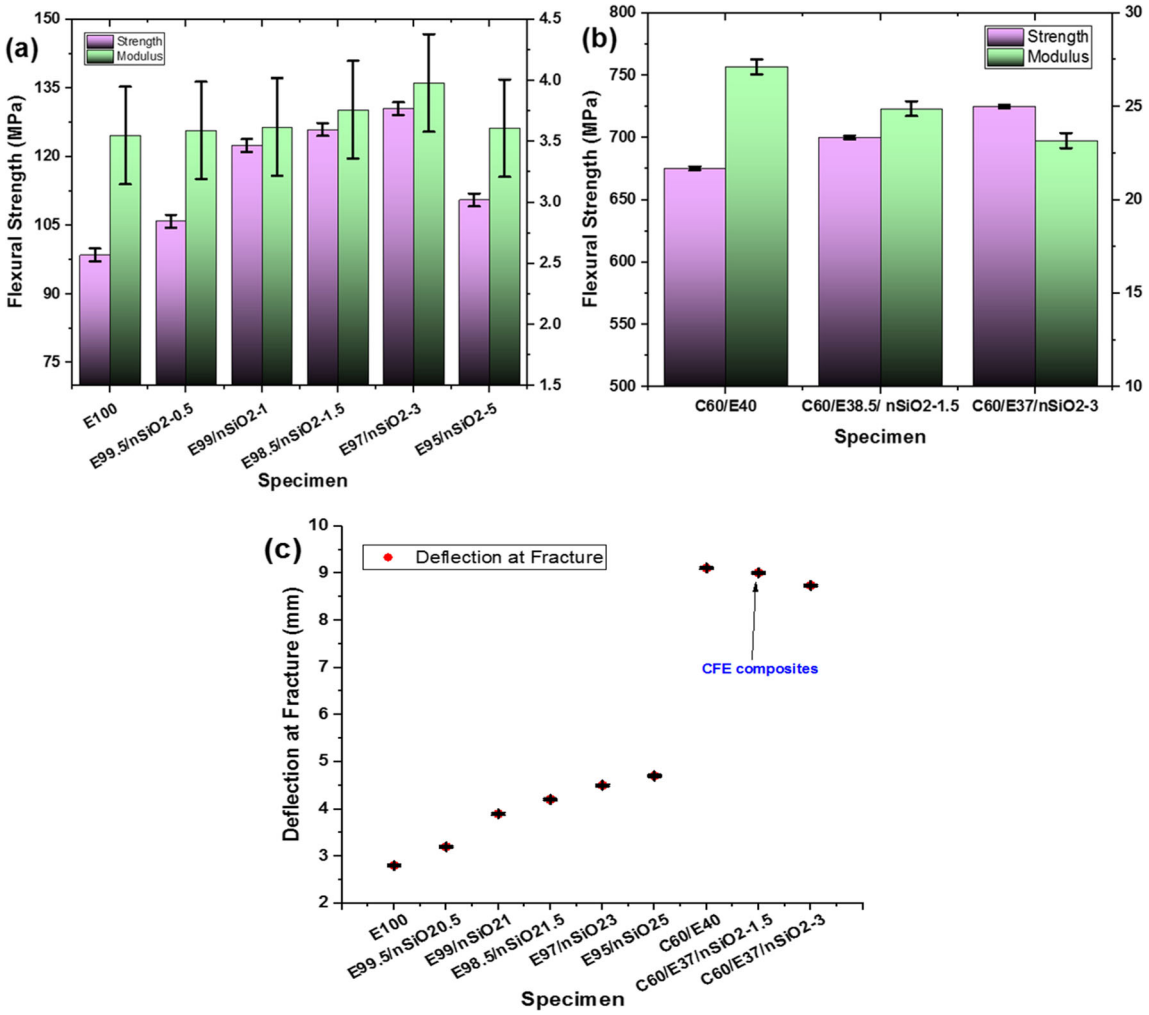

Fig. 6 Flexural properties of the composites: **a** Epoxy/nSiO_2 mono composites, **b** CFE/nSiO_2 hybrid composites, **c** Deflection at fracture load of all composites

by many parameters like nanoparticle geometry, the extension of dispersion, the surface area of the nanoparticles (size), and method of dispersion and so on [10, 21, 50–52]. In this section, the discussion is made in two segments. Primarily, with nSiO_2/Ep mono composites and secondly, with nSiO_2/CFE hybrid composites. The nSiO_2/Ep mono composite consists of two-phases where, we can see the agglomeration effect with the E95/nSiO_2–5. However, the size of the particle aggregation is different in both the composites. The aggregates in the E97/nSiO_2–3 nanocomposites still managed to be in nanometer dimensions. Figure 9a shows the TEM micrograph of the E97/nSiO_2–3 where the dispersion is nearly uniform. Figure 9b shows the TEM micrograph of E95/nSiO_2–5, the nSiO_2 is still in well dispersed phase. These aggregates are in micron size range. This makes the particles to reduce material strength. Figure 9c shows the TEM micrograph of the neat epoxy matrix. The extent of the dispersion depends on the process that will be used for the dispersion of the nanoparticles. There are many processes available for the dispersion of nanoparticles from manual stirring to three-roll mill. In this study we have used the ultrasonication process along with a few pre and post processing (refer fabrication section). Sapiai et al. have used mechanical mixing [19]. Zheng et al. have studied ultrasonication and high speed homogenization at 24000 rpm [20] Chen et al. have used the solvent dissolution and the ultrasonication [21]. Zheng et al. have used only high speed homogenization for the dispersion of nSiO_2 [20].

The energy dispersive analysis of X-rays was performed on 5 wt.% of SiO_2 composites at the zone with higher agglomeration. The major portion of the elemental share goes to oxygen with 45.08% in the entire scanning region. However, oxygen is shared between two elements they are carbon and silicon. The total share of carbon is 34.09% and silicon is 14.28%. Other elements found are sodium with 4.17% and sulphur of 2.39%. All these percentage contributions mentioned in here are based on the weight percentage of all the elements present in the scanning region. The observation that needs to be done here is that the maximum nSiO_2 reinforcements used with epoxy are 5 wt.%. If uniform distribution were to be present then the percentage by weight contribution should have been

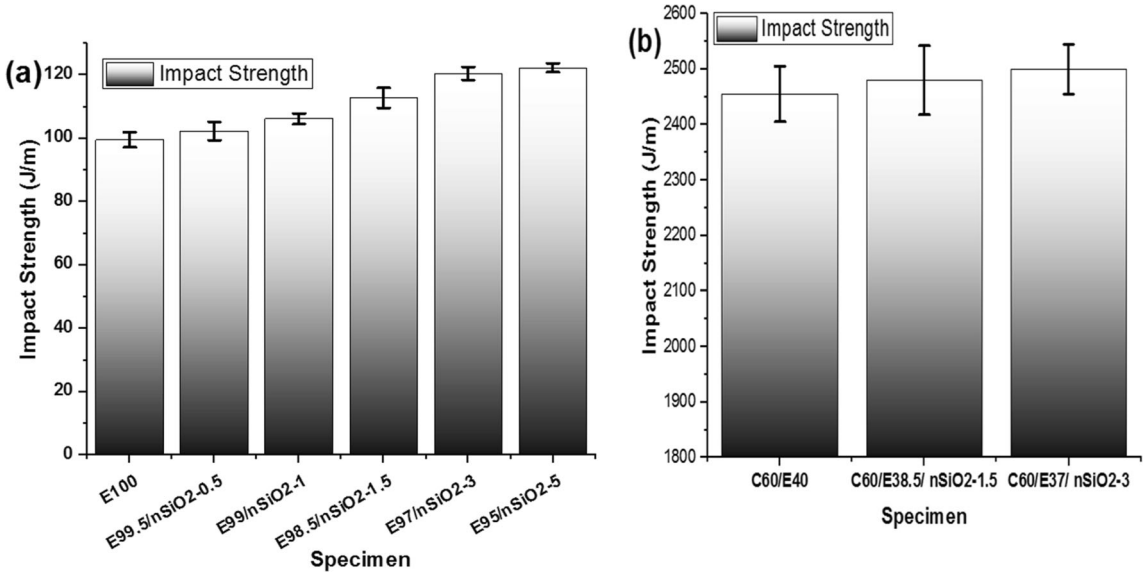

Fig. 7 Impact properties of the composites: **a** Epoxy/nSiO_2 mono composites, **b** CFE/nSiO_2 hybrid composites

much closer to 5 wt.%. However, this scanning region has the overall content of silicon to be 14% by weight. Figure 9d shows the EDAX elemental peak plot for E95/nSiO_2–5. Table 4 shows the percentage contribution of the each element.

The nSiO_2 is added in a small quantities and extended till 5 wt.%. From the tensile and flexural results, it can be seen that till 3 wt.% of the nSiO_2 with epoxy the strength got enhanced. This enhancement can be attributed to the dispersion of the nanoparticles and the interfacial adhesion of the particles. The nanoparticles were silane treated that enhanced the adhesion between the nanoparticles and the matrix material. The benefit of the improved interfacial adhesion is that there will be proper stress transfer between the matrix and nanoparticles. In parallel, uniformity in dispersion also helps to have the uniform stress transfer throughout the specimen. Upon the formation of the agglomeration in the n-SiO_2/Ep system, the reduction in the adhesion between the particles and the matrix material offer the path of the least resistance hence the reduction in the strength can be observed. In the

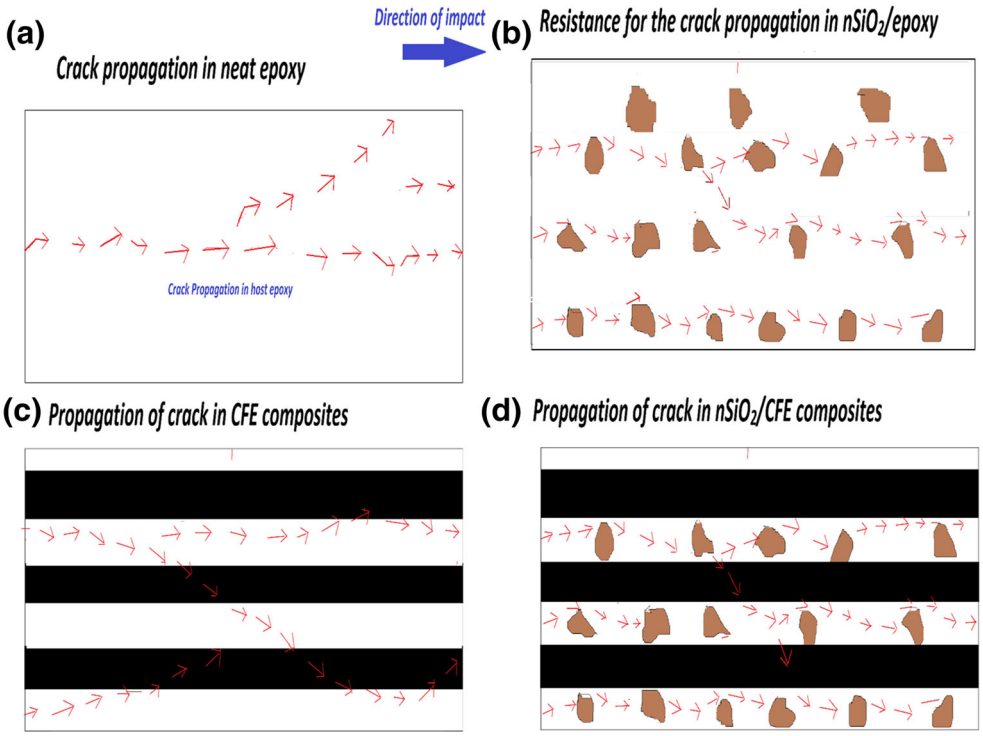

Fig. 8 Crack propagation mechanism through different layer of the composites: **a** neat epoxy, **b** nSiO_2/Ep mono composites, **c** unfilled CFE and (d) nSiO_2/CFE hybrid composites

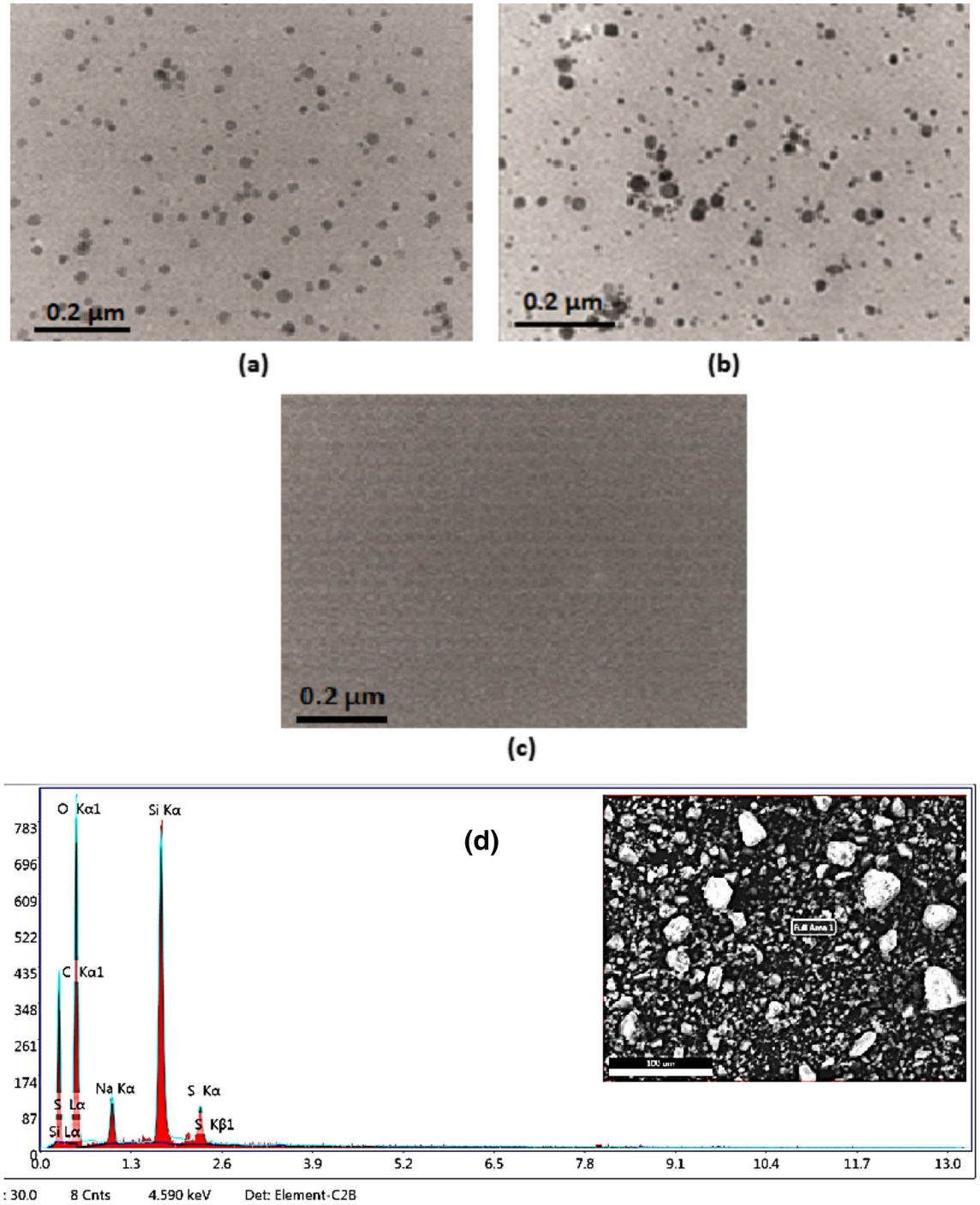

Fig. 9 The TEM images of: **a** E97/nSiO$_2$–3, **b** E95/nSiO$_2$–5, **c** Neat epoxy, and **d** EDAX elemental plot for E95/nSiO$_2$–5

Table 4 Contribution of different elements in E95/nSiO$_2$–5 mono composites

Elements	Percentage sharing
Carbon	34.09%
Oxygen	45.08%
Silicon	14.28%
Sodium	4.17%
Sulphur	2.39%

lower content of the nSiO$_2$, the material may induce a certain micro cracks that will tend to act as a stress concentration region. However, these micro-cracks also induce the localised plastic deformation that will make the cracks to diverge onto the different path altogether. Further, increase in the nSiO$_2$ loading, these micro-cracks growth and the localised plastic deformations increases. These micro-cracks when diverge and orient in the direction orthogonal to direction of fracture then

this will be able to absorb much more energy when compared to the specimens where the micro-crack are oriented parallel to the specimen fracture direction. Similar phenomenon is also observed by Xiao et al. [40]. Similarly, for the $nSiO_2$/CFE composites the silane treatment on fiber as well as on the $nSiO_2$ improved the adhesion of the reinforcements with epoxy matrix. This is discussed in the further sections.

3.5.2 Fractography of the Tensile Test Fractured Specimens of CFE Hybrid Composites

The fractured surface morphology of the CFE composites and $nSiO_2$/CFE tested tensile composites were observed under the scanning electron microscope and noted that the matrix was squeezed well between the fabric layers and the fibers. The matrix usually transfers the load on to fiber and acts as structural support for fibers that enhance the strength of the material in total. During loading, the specimen is pulled and the elongation of the specimen takes place. This elongation initiates cracks in the material and the brittleness of the epoxy will tend to propagate the locally generated crack during elongation. This leads to the removal of a portion of the matrix around the fibers. This constitutes for the fiber de-bonding. As the fiber is debonded, it gradually loses its ability to carry the load and thus reduces the material strength.

From Fig. 10a, it can be observed that the fiber de-bonding and fiber drags. Both the phenomena signify the improper fiber/epoxy bonding. The magnified image in Fig. 10b shows that the local cracks that lead to the early failure of the material. The crystalline behaviour of the material is observed with the unfilled CFE composites. However, the superficial fiber-matrix bonding is observed in the composites with $nSiO_2$ reinforcement. It can be seen that the $nSiO_2$ filled has also helped to squeeze between the fibers that make the $nSiO_2$ particles participate in the load-bearing event. From Fig. 10c, it is clear that the fiber de-bonding has significantly reduced and the fiber pullouts are not visible. Hence, the $nSiO_2$ can also benefit from improving the load-bearing capacity. Figure 10d, shows the magnified image of the failed specimen depicts the amorphous nature that was introduced upon reinforcing the nSiO2.

3.5.3 Fractography of the Flexural Test Fractured Specimens of CFE Hybrid Composites

The Bending test portrayed significant improvement in flexural properties upon adding nanoparticles with CFE. From Fig. 11a the weak fiber/matrix bonding was noted. The fibers are cut almost diametrically, which affirms the brittleness of the CFE composites. Due to the brittleness of the epoxy material, the fibers undergo failure along with the matrix material forming the diametrical failure. In addition, it can be seen that

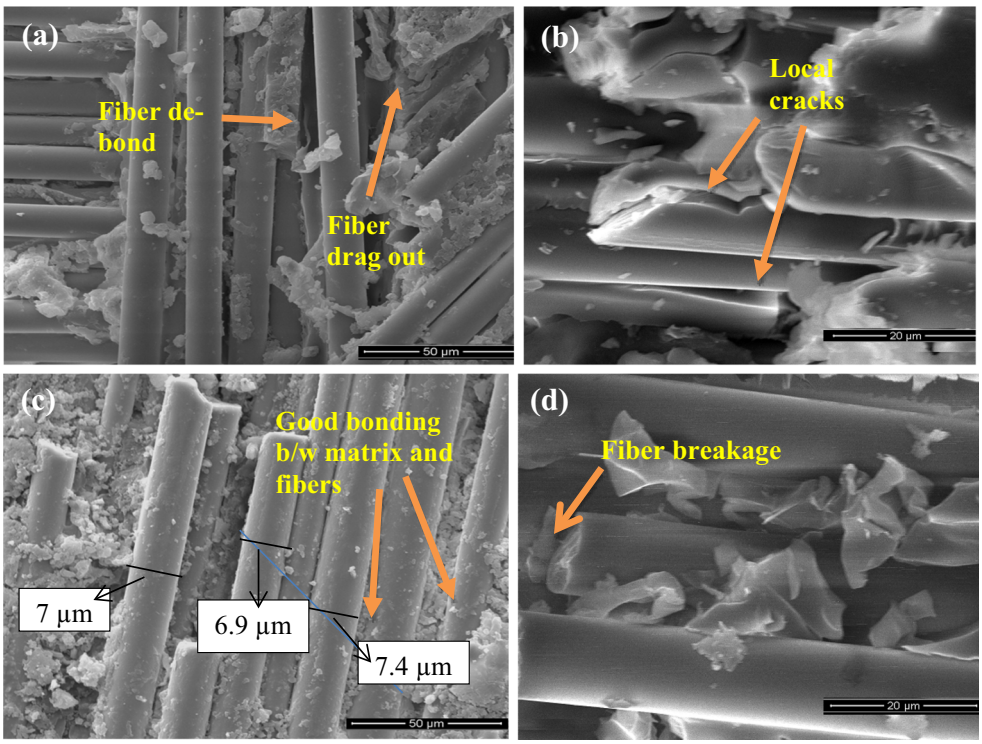

Fig. 10 The SEM images of the fractured tensile specimens: **a** CFE composite, lower magnification, **b** CFE composite, higher magnification, **c** C60/E37/$nSiO_2$–3 composite, lower magnification, **d** C60/E37/$nSiO_2$–3 higher magnification

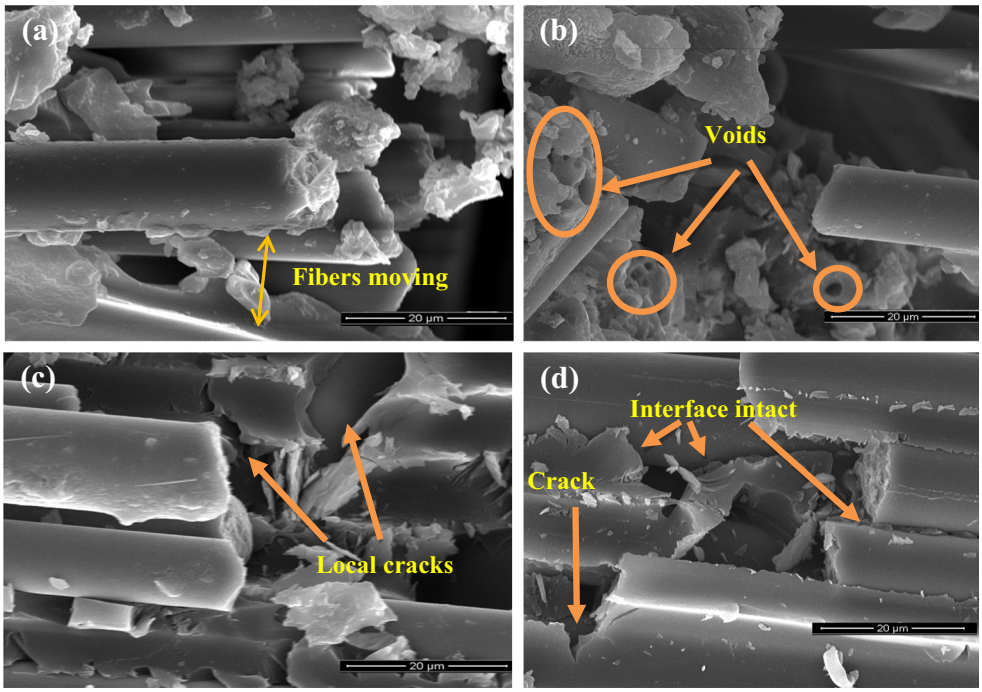

Fig. 11 The SEM images of the fractured flexural specimens: **a** CFE composite, lower magnification, **b** CFE composite, higher magnification, **c** C60/E37/$nSiO_2$–3 composite, lower magnification, **d** C60/E37/$nSiO_2$–3 higher magnification

the epoxy failed to penetrate between the fibers thus causing reduced strength. Figure 11b portrays the presence of micro-voids in the material. As the void content increases in the material, properties are deteriorated [12, 22]. On the other hand, an increased deflection and localized cracks made the fibers to get detached from the fiber/matrix interface. These cracks can be observed in Fig. 11c and d. The evidence for the superficial fiber matrix is provided in Fig. 11d. It is seen that the matrix material was well squeezed between the fibers benefitting to keep the fibers intact. This is responsible for the improvement in the property. However, the voids found in the material without $nSiO_2$ are minimized in the $nSiO_2$/CFE composites.

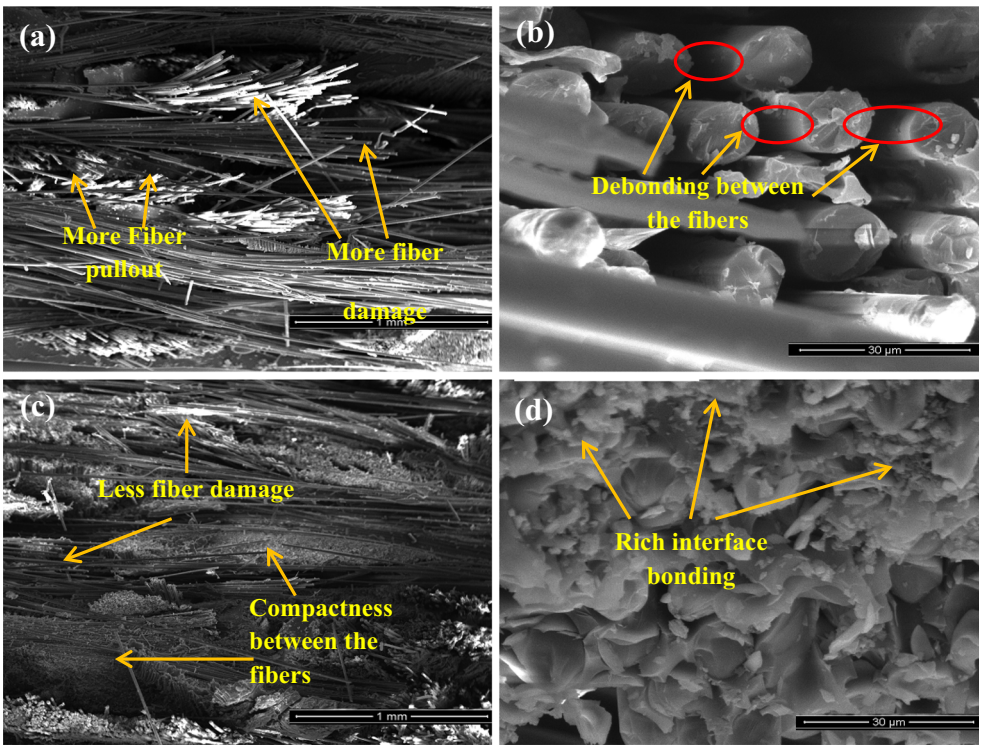

Fig. 12 The SEM images of the fractured impact specimen: **a** CFE composite, lower magnification, **b** CFE composite, higher magnification, **c** C60/E37/$nSiO_2$–3 composite, lower magnification, **d** C60/E37/$nSiO_2$–3 higher magnification

3.5.4 Fractography of the Test Failed Specimens of CFE Hybrid Composites

The impact tests were performed on the materials to evaluate the impact toughness of the material. The increment in the properties was observed though it is not so substantial. From Fig. 12a the long fibers are visible that indicated that the impact energy on to composites was poorly transferred through the fibers in the CFE composites. Hence, the debonding of the fibers was observed. The closer observation shown in Fig. 12b of the fibers that failed at the junction, shows the debonded fibers with each other due to lack of interface interaction. Embedded epoxy around the fiber surface was removed when impact load was applied. The impact energy fractured the fibers at an angle. With the introduction of nSiO2, the composite behaved totally in a different way. In Fig. 12c improved adhesion between the constituents of the composite was noticed due to the addition of $nSiO_2$ particles. Figure 12d illustrates the magnified view of the fractured cross-section of $nSiO_2$/CFE hybrid composite. The amorphous nature of the matrix with the other elements was also noted. However, the key point to be noticed here in this picture is that the fibers failed orthogonal to the longitudinal axis.

4 Conclusions

In this investigation, the mechanical properties of the epoxy-based composites with and without carbon fiber and the silane agent treated $nSiO_2$ were investigated according to the ASTM standards and considerable enhancement in the properties was observed. Based on the observations, the following conclusions were derived.

- The enhancement in density of the composites can be attributed to higher densities of the reinforcements. However, the void content was increased in non-fibrous composites and the same has decreased in $nSiO_2$/CFE composites. This affirms that the $nSiO_2$ composites was well blended and filled in the empty spaces and proper degasification.
- The hardness of the composites had an increment trend in both non-fibrous $nSiO_2$ and $nSiO_2$/CFE composites is due to the crosslinking of the silane treated $nSiO_2$ and epoxy and uniformity in dispersion of particles.
- The tensile and flexural properties were enhanced with the addition of $nSiO_2$ in both non-fibrous and CFE composites till 3 wt.% filler loading. 3 wt.% loading was found to be the optimal loading for the $nSiO_2$ which coincides with the previous literature. The impact strength of $nSiO_2$/Epoxy and $nSiO_2$/CFE composites also improved with the addition of $nSiO_2$.
- The Scanning electron micrographs of the E95/$nSiO_2$–5 revealed the formation of SiO_2 aggregates that extend to the dimension up to 5 μm. This justifies the reduction in the properties at 5 wt.% of the composites. The fractured surface of tensile, flexural, and impact coupons were analyzed using scanning electron micrographs.
- The improvement in the properties was associated with better interfacial adhesion between matrix and reinforcements in both $nSiO_2$/Epoxy and $nSiO_2$/CFE composites and the reduction in void content is an added advantage in the case of CFE composites.

Acknowledgements National Institute of Engineering, Centre for Research & Development (NIE-CRD) and TEQIPIII, NPIU funded this work. The authors would like to acknowledge the support of the Board of Management, NIE, Principal, and TEQIP-III Coordinator. The Universal testing machine was procured from Kalpak Instruments and Controls, Pune, Mumbai. India. We would like to extend our sincere gratitude to Mr. SK Sidhaye (CEO), Kalpak Instruments and Controls. Thanks go to the following Centre for Composite Materials Research (CCMR), NIE, technical staff Mr. Byresh for the help rendered in conducting experiments.

Compliance with Ethical Standards

Conflict of Interest The authors declare that there are no such conflicts of interest regarding the publication of this paper.

References

1. Irez AB, Bayraktar E, Miskioglu I (2020) Fracture toughness analysis of epoxy-recycled rubber-based composite reinforced with graphene nanoplatelets for structural applications in automotive and aeronautics. Polymers 12:448
2. Nayak SK, Mohanty S, Nayak SK (2020) Thermal, electrical and mechanical properties of expanded graphite and micro-SiC filled hybrid epoxy composite for electronic packaging applications. J Electron Mater 49:212–225
3. Chen J, Lekawa-Raus A, Trevarthen J, Gizewski T, Lukawski D, Hazra K, Rahatekar SS, Koziol KK (2020) Carbon nanotube films spun from a gas phase reactor for manufacturing carbon nanotube film/carbon fibre epoxy hybrid composites for electrical applications. Carbon 158:282–290
4. Kuruvilla SP, Renukappa NM, Suresha B (2020) Dynamic mechanical properties of glass fiber reinforced epoxy composites with micro and nanofillers. InTechno-Societal 2018:337–347 Cham: Springer
5. Siddalingappa SK, Pal B, Haseebuddin MR, Gopalakrishna K (2020) Tribological behaviour of carbon fibre polymer composites reinforced with nano-fillers. Int Adv Appl Mechan Eng 2020:791–800 Springer, Singapore
6. Hou L, Gao J, Ruan H, Xu X, Lu S (2020) Mechanical and thermal properties of hyperbranched poly (ε-caprolactone) modified graphene/epoxy composites. J Polym Res 27(2):32
7. Nanda BP, Satapathy A (2020) Thermal, acoustic, and dielectric behaviour of epoxy-based hybrid composites using short hair fiber. J Braz Soc Mech Sci Eng 42:1–2
8. Toorchi D, Tohidlou E, Khosravi H (2020) Enhanced flexural and tribological properties of basalt fiber-epoxy composite using nano-

zirconia/graphene oxide hybrid system. J Ind Text. https://doi.org/10.1177/1528083720920573
9. Alsaadi M, Erkliğ A (2019) Effects of clay and silica nanoparticles on the Charpy impact resistance of a carbon/aramid fiber reinforced epoxy composite. Mater Test 61:65–70
10. Suresha B, Hemanth G, Hemanth R, Lalla NP (2020) Role of graphene nanoplatelets and carbon fiber on mechanical properties of PA66/thermoplastic copolyester elastomer composites. Mater Res Exp 7(1):015325
11. Zhaohong X, Zhenhua L, Jian L, Fei FY (2014) The effect of CF and nano-SiO_2 modification on the flexural and tribological properties of POM composites. J Thermoplast Compos Mater 27(3): 287–296
12. Zhu H, Wu B, Li D, Zhang D, Chen Y (2011) Influence of voids on the tensile performance of carbon/epoxy fabric laminates. J Mater Sci Technol 27(1):69–73
13. Bilisik K, Karaduman N, Sapanci E (2020) Short-beam shear of nanoprepreg/nanostitched three-dimensional carbon/epoxy multiwall carbon nanotube composites. J Compos Mater 54:311–329
14. Kaybal HB, Ulus H, Demir O, Şahin ÖS, Avcı A (2018) Effects of alumina nanoparticles on dynamic impact responses of carbon fiber reinforced epoxy matrix nanocomposites. Eng Sci Technol Int J 21(3):399–407
15. Nallusamy S (2016) Characterization of epoxy composites with TiO_2 additives and E-glass fibers as reinforcement agent. Int J Nano Res 40:99–104 Trans Tech Publications Ltd.
16. Kwon DJ, Shin PS, Kim JH, Baek YM, Park HS, DeVries KL, Park JM (2017) Interfacial properties and thermal aging of glass fiber/epoxy composites reinforced with SiC and SiO_2 nanoparticles. Compos Part B Eng 130:46–53
17. Yang J, Wang C, Zeng J, Jiang D (2018) Effects of nano-SiO_2 on mechanical and hygric behaviours of glass fiber reinforced epoxy composites. Sci Eng Compos Mater 25(2):253–259
18. Ahmad T, Mamat O, Ahmad R (2013) Studying the effects of adding silica sand nanoparticles on epoxy based composites. J Nanoparticles 1:1–5
19. Sapiai N, Jumahat A, Manap N, Usoff MA (2015) Effect of nanofillers dispersion on mechanical properties of clay/epoxy and silica/epoxy nanocomposites. J Teknol 76(9):107–111
20. Zheng Y, Zheng Y, Ning R (2003) Effects of nanoparticles SiO_2 on the performance of nanocomposites. Mater Lett 57(19):2940–2944
21. Chen L, Chai S, Liu K, Ning N, Gao J, Liu Q, Chen F, Fu Q (2012) Enhanced epoxy/silica composites mechanical properties by introducing graphene oxide to the interface. ACS Appl Mater Interfaces 4(8):4398–4404
22. Jeong H (1997) Effects of voids on the mechanical strength and ultrasonic attenuation of laminated composites. J Compos Mater 31(3):276–292
23. Zhu JB, Yang XJ, Cui ZD, Zhu SL, Wei Q (2006) Preparation and properties of nano-SiO_2/epoxy composites cured by Mannich amine. J Macromol Sci Part B 45(5):811–820
24. Liu S, Zhang H, Zhang Z, Sprenger S (2009) Epoxy resin filled with high volume content nano-SiO_2 particles. J Nanosci Nanotechnol 9(2):1412–1417
25. Zhang T, Zhang L, Li C (2011) Study of the preparation and properties of PBT/epoxy/SiO_2 nanocomposites. J Macromol Sci Part B 50(5):967–974
26. Nikje MM, Khanmohammad M, Garmarudi AB, Ghasemi K (2008) Analysis of variance (ANOVA) for optimizing the nano-SiO_2 content of high performance epoxy nanocomposites. J Macromol Sci Part A 46(1):116–120
27. Gao J, Li J, Zhao S, Benicewicz BC, Hillborg H, Schadler LS (2013) Effect of graft density and molecular weight on mechanical properties of rubbery block copolymer grafted SiO2 nanoparticle toughened epoxy. Polymer. 54(15):3961–3973
28. Zhang G, Rasheva Z, Karger-Kocsis J, Burkhart T (2011) Synergetic role of nanoparticles and micro-scale short carbon fibers on the mechanical profiles of epoxy resin. Express Polym Lett 5(10):859–872
29. Feli S, Jalilian MM (2016) Experimental and optimization of mechanical properties of epoxy/nanosilica and hybrid epoxy/fiberglass/nanosilica composites. J Compos Mater 50:3891–3903
30. Yao XF, Zhou D, Yeh HY (2008) Macro/microscopic fracture characterizations of SiO2/epoxy nanocomposites. Aerosp Sci Technol 12(3):223–230
31. Fu J, Zhang M, Jin L, Liu L, Li N, Shang L, Li M, Xiao L, Ao Y (2019) Enhancing interfacial properties of carbon fibers reinforced epoxy composites via layer-by-layer self-assembly GO/SiO_2 multilayers films on carbon fibers surface. Appl Surf Sci 470:543–554
32. Lew C, Chowdhury F, Hosur MV, Netravali AN (2007) The effect of silica (SiO_2) nanoparticles and ammonia/ethylene plasma treatment on the interfacial and mechanical properties of carbon-fiber-reinforced epoxy composites. J Adhes Sci Technol 21(14):1407–1424
33. Zegaoui A, Derradji M, Ma R, Cai WA, Medjahed A, Liu WB, Dayo AQ, Wang J (2018) Silane-modified carbon fibers reinforced cyanate ester/benzoxazine resin composites: morphological, mechanical and thermal degradation properties. Vacuum. 1(150):12–23
34. Jawaid M, Khalil HA, Bakar AA, Khanam PN (2011) Chemical resistance, void content and tensile properties of oil palm/jute fibre reinforced polymer hybrid composites. Mater Des 32(2):1014–1019
35. Liu L, Zhang BM, Wang DF, Wu ZJ (2006) Effects of cure cycles on void content and mechanical properties of composite laminates. Compos Struct 73(3):303–309
36. Raju BR, Suresha B, Swamy RP, Bharath KN (2012) The effect of silicon dioxide filler on the wear resistance of glass fabric reinforced epoxy composites. Adv Polym Sci Technol 2(4):51–57
37. Anjum N, Ajit Prasad SL, Suresha B (2013) Role of silicon dioxide filler on mechanical and dry sliding wear behaviour of glass-epoxy composites. Adv Tribol 1:1–10
38. Yadaw RC, Chaturvedi S (2012) An investigation of mechanical and sliding wear behaviour of glass fiber reinforced polymer composite with or without addition of silica. International Conference on PFAM XXI, IIT Guwahati
39. Ahmed FJ (1990) A review of particulate reinforcement theories for polymer composites. J Mater Sci 25:4933–4942
40. Xiao C, Tan Y, Yang X, Xu T, Wang L, Qi Z (2018) Mechanical properties and strengthening mechanism of epoxy resin reinforced with nano-SiO_2 particles and multi-walled carbon nanotubes. Chem Phys Lett 695:34–43
41. Kaybal HB, Ulus H, Demir O, Tatar AC, Avcı A (2017) Investigations on the mechanical properties of the nano SiO_2 epoxy nanocomposite. Appl Eng Lett 2(4):121–124
42. Suresha B, Saini MS (2016) Influence of organo-modified montmorillonite nanolayers on static mechanical and dynamic mechanical behaviour of carbon/epoxy composites. J Compos Mater 50: 3589–3601
43. Zhou Y, Jeelani S, Lacy T (2014) Experimental study on the mechanical behavior of carbon/epoxy composites with a carbon nanofiber-modified matrix. J Compos Mater 48:3659–3672
44. Pascoe KJ (1978) An introduction to the properties of engineering materials3rd edn. Van Nostrand Reinhold, London
45. Eslami-Farsani R, Khosravi H (2017) On the flexural properties of multiscale nanosilica/E-glass/epoxy anisogrid-stiffened composite panels. J Comput Appl Res Mech Eng 7:99–108
46. Cao Y, Cameron J (2006) Flexural and shear properties of silica particle modified glass fiber reinforced epoxy composite. J Reinf Plast Compos 25:347–359
47. Lu SR, Zhang HL, Wang XY (2005) Wear and mechanical properties of epoxy/SiO 2-TiO 2 composites. J Mater Sci 40:2815–2821

48. Zheng Y, Ning R, Zheng Y (2005) Study of SiO_2 nanoparticles on the improved performance of epoxy and fiber composites. J Reinf Plast Compos 24:223–233
49. Safi S, Zadhoush A, Ahmadi M (2017) Flexural and Charpy impact behaviour of epoxy/glass fabric treated by nano-SiO_2 and silane blend. Plast Rubber Compos 46:314–321
50. Alishahi E, Shadlou S, Doagou-R S, Ayatollahi MR (2013) Effects of carbon nano reinforcements of different shapes on the mechanical properties of epoxy-based nanocomposites. Macromol Mater Eng 298(6):670–678
51. Ahmad FN, Jaafar M, Palaniandy S, Azizli KA (2008) Effect of particle shape of silica mineral on the properties of epoxy composites. Compos Sci Technol 68(2):346–353
52. Fu SY, Feng XQ, Lauke B, Mai YW (2008) Effects of particle size, particle/matrix interface adhesion and particle loading on mechanical properties of particulate–polymer composites. Compos Part B: Eng 39(6):933–961